Science Advances
AAAS

Supplementary Materials for

Therapeutic implications of mitochondrial stress–induced proteasome inhibitor resistance in multiple myeloma

Aditi Sharma *et al.*

Corresponding author: Mala Shanmugam, mala.shan@emory.edu

Sci. Adv. **8**, eabq5575 (2022)
DOI: 10.1126/sciadv.abq5575

The PDF file includes:

Other Supplementary Material for this manuscript includes the following:

Fig S1

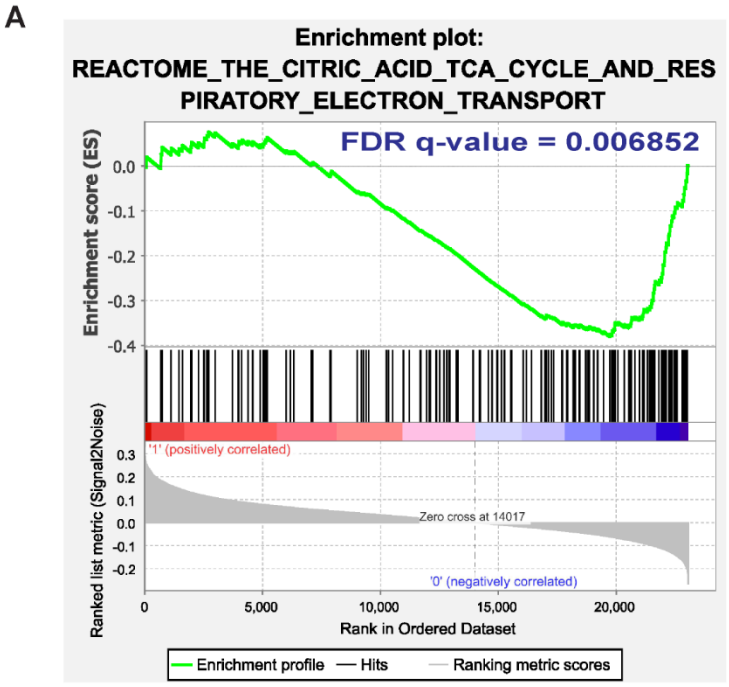

Fig. S1. TCA cycle and respiratory electron transport chain REACTOME pathway is downregulated in patients with PFS < 2 yrs in the CoMMpass trial. (A) Enrichment plot of the citric acid TCA cycle and respiratory electron transport chain REACTOME pathway generated from GSEA performed in MM patients from the CoMMpass trial (NCT0145429) with poor prognosis (PFS < 2 yrs., n = 426) vs. patients with better prognosis (PFS > 2 yrs., n = 341).

Fig S2

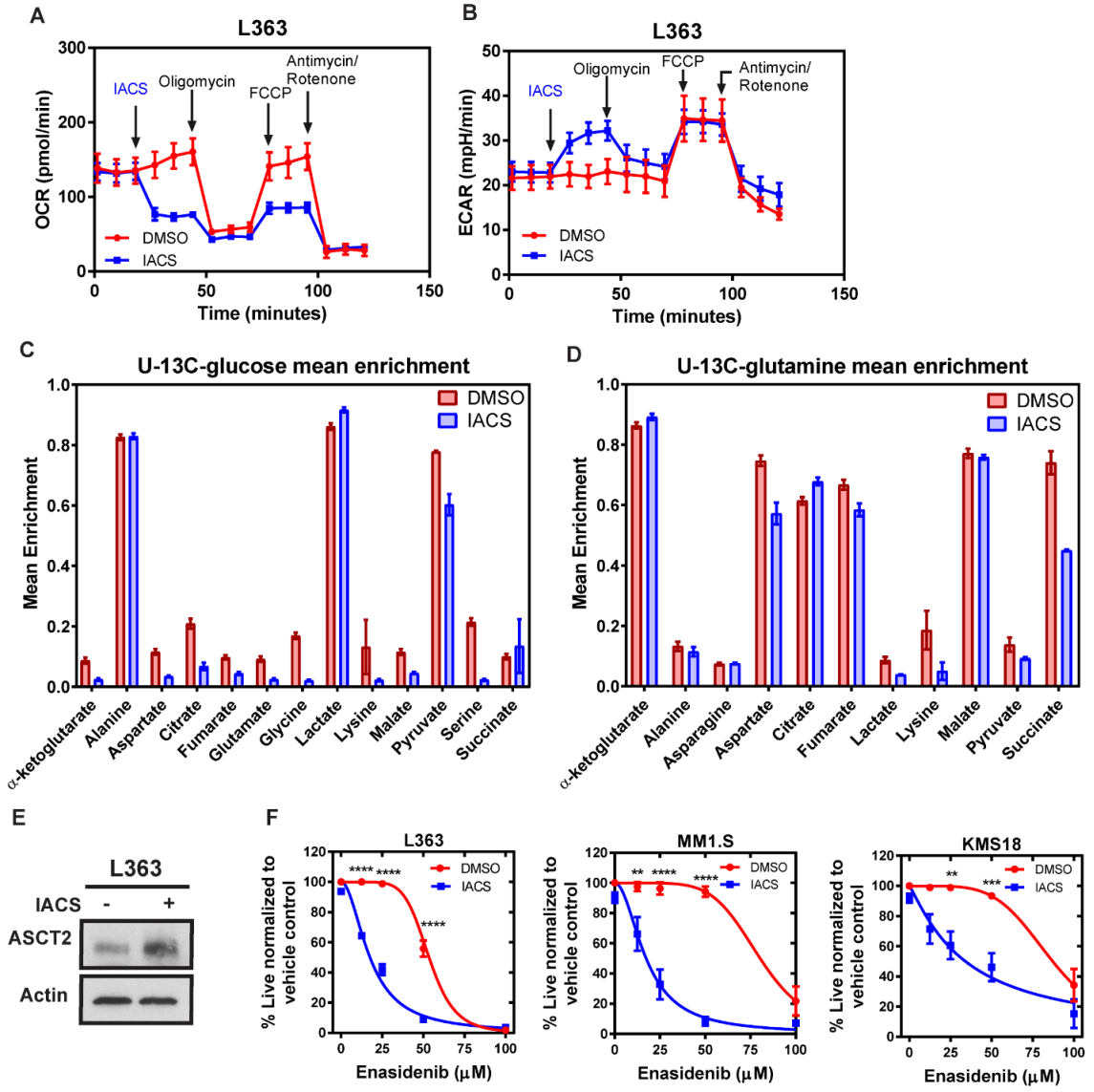

Fig. S2. Complex I inhibition alters cellular energetics and amino acid homeostasis and sensitizes MM to enasidenib. (A) OCR and **(B)** ECAR were determined in L363 cells after acute DMSO or IACS injection. Data are presented as mean values +/- SEM. **(C)** U-13C-glucose mean enrichment measured in DMSO and IACS treated L363 cells, supplemented with U-13C-glucose for 9 h (n = 3). Data are presented as mean values +/- SD. **(D)** U-13C-glutamine mean enrichment measured in DMSO and IACS treated L363 cells, supplemented with U-13C-glutamine for 9 h (n = 3). Data are presented as mean values +/- SD. **(E)** L363 cells treated with IACS (25 nM) for 24 h were evaluated for expression of ASCT2 by immunoblot analysis with actin as loading control. **(F)** Dose response curves for co-treatment of L363, MM.1S and KMS18 cells with 25nM IACS and increasing doses of enasidenib for 24 h. Data are represented as mean ± SEM (n = 3). All cell viability was assessed by AnnexinV/DAPI flow cytometric staining.

Fig S3

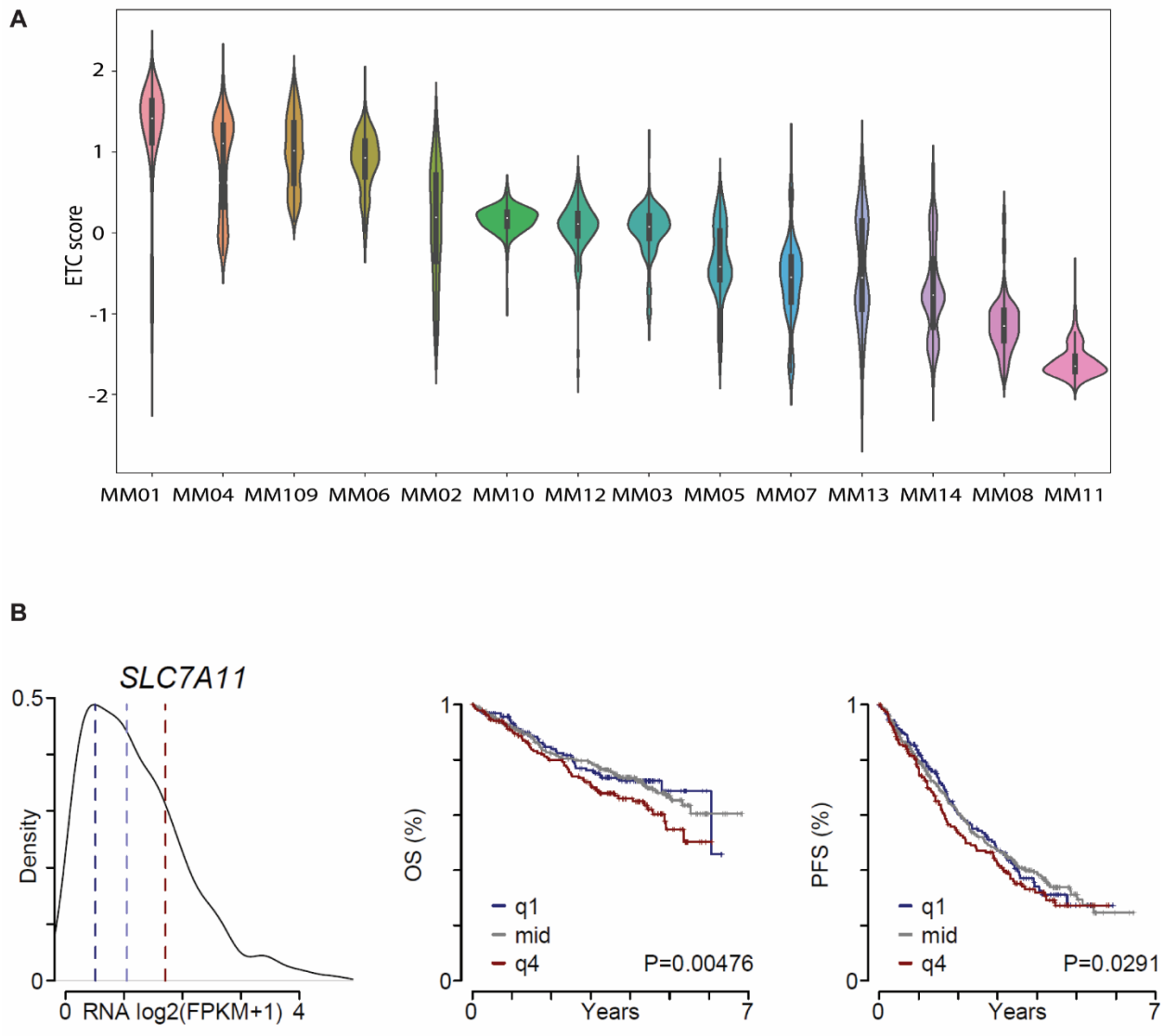

Fig. S3. MM exhibits heterogeneity in ETC gene expression. (A) Violin plots of ETC score of MM patients vs normal donors. ETC score generated from sc-RNA seq analysis of MM cells using GSE11756 (as described in Methods). **(B)** (left) Expression of SLC7A11 in newly diagnosed samples from the CoMMpass study (N=768), with first, second, and third quartiles denoted by blue, gray, and red, dashed vertical lines, respectively. Association of SLC7A11 expression and OS (middle) and PFS (right) in CoMMpass patients with patients stratified by SLC7A11 expression into a low quartile (q1, blue), the two middle quartiles (mid, gray), and high quartile (q4, red). Significance was determined using a Cox proportional hazards model with a Wald's test where gene expression was treated as a quantitative response.

Fig S4

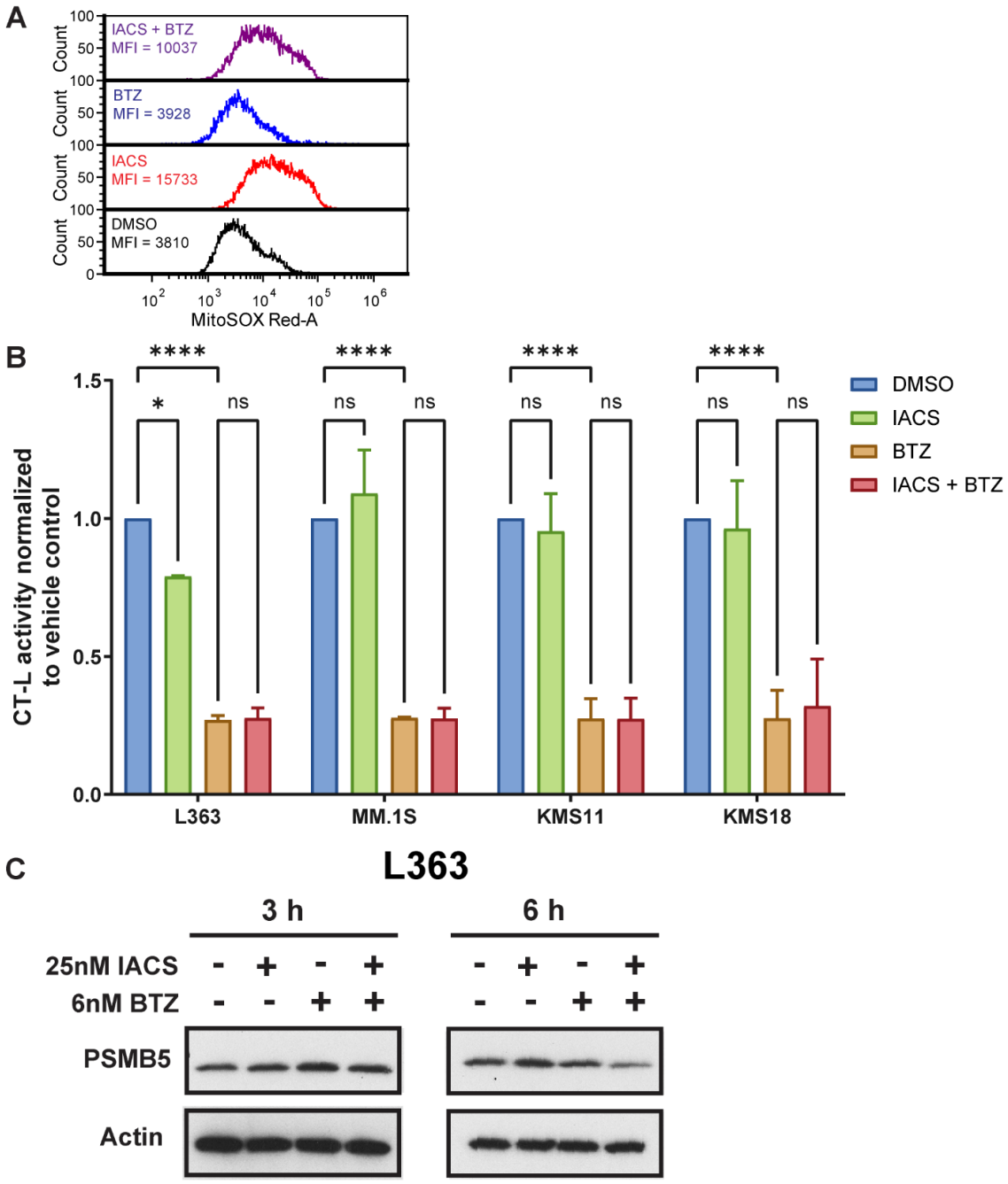

Fig. S4. Proteasome is inhibited in cells treated with IACS + BTZ. (A) Cellular ROS levels measured in L363 cells treated with 25nM IACS +/- 6nM BTZ for 24 h using CellROX Deep Red. One representative experiment in shown (n = 3). **(B)** Chymotrypsin like (CT-L) activity of proteasomes was measured in L363, MM.1S, KMS11 and KMS18 cells treated with 25nM IACS and 6nM BTZ for 3h using fluorogenic substrate Suc-LLVY-AMC. Data are presented as mean values +/- SD. Adjusted p values are calculated using a two-way ANOVA with post-hoc Tukey's multiple comparisons test. **(C)** L363 treated with IACS (25 nM) for 3 and 6 hrs evaluated for expression of PSMB5 by immunoblot analysis.

Fig S5

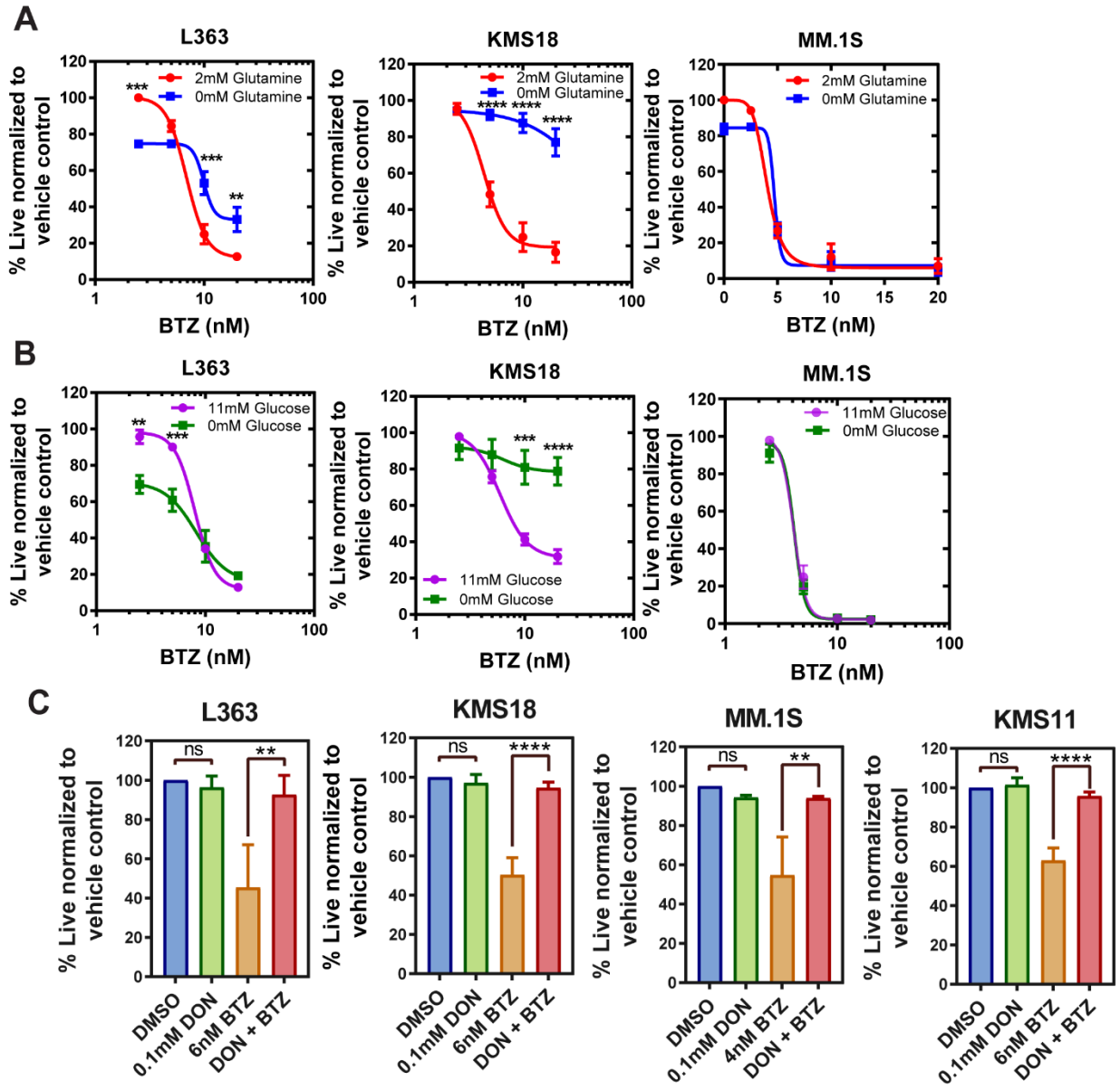

Fig. S5. Glutamine deprivation and glutamine antagonist DON treatment antagonize BTZ-induced apoptosis. BTZ dose-response curves for L363, KMS18 and MM.1S cells cultured with and without glutamine **(A)** or with or without glucose **(B)** and increasing doses of BTZ for 24 h. **(C)** L363, MM.1S, KMS11 and KMS18 cells treated with BTZ and 0.1mM DON for 24 h. (n = 3). Data are presented as mean values +/- SD. p-values are calculated using two-tailed t-tests with Welch's correction. All viability was assessed by AnnexinV/DAPI flow cytometric staining.

Fig S6

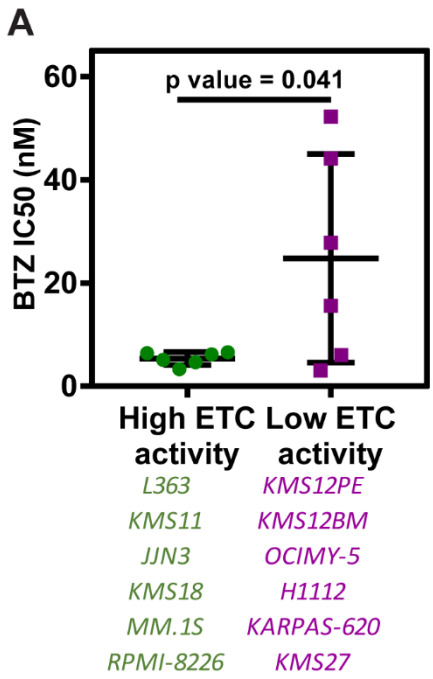

Fig S6: MM cell lines demonstrate differential sensitivity to bortezomib inversely correlating with ETC activity. (A) BTZ IC50 values for MM cell lines with high and low ETC activity (as previously reported) determined using a CellTiter-Glo assay. P value is calculated using a two-tailed t-test. The ETC activities (Complex I and II activities and mitochondrial oxygen consumption rates) were previously reported by us (23).

Fig S7

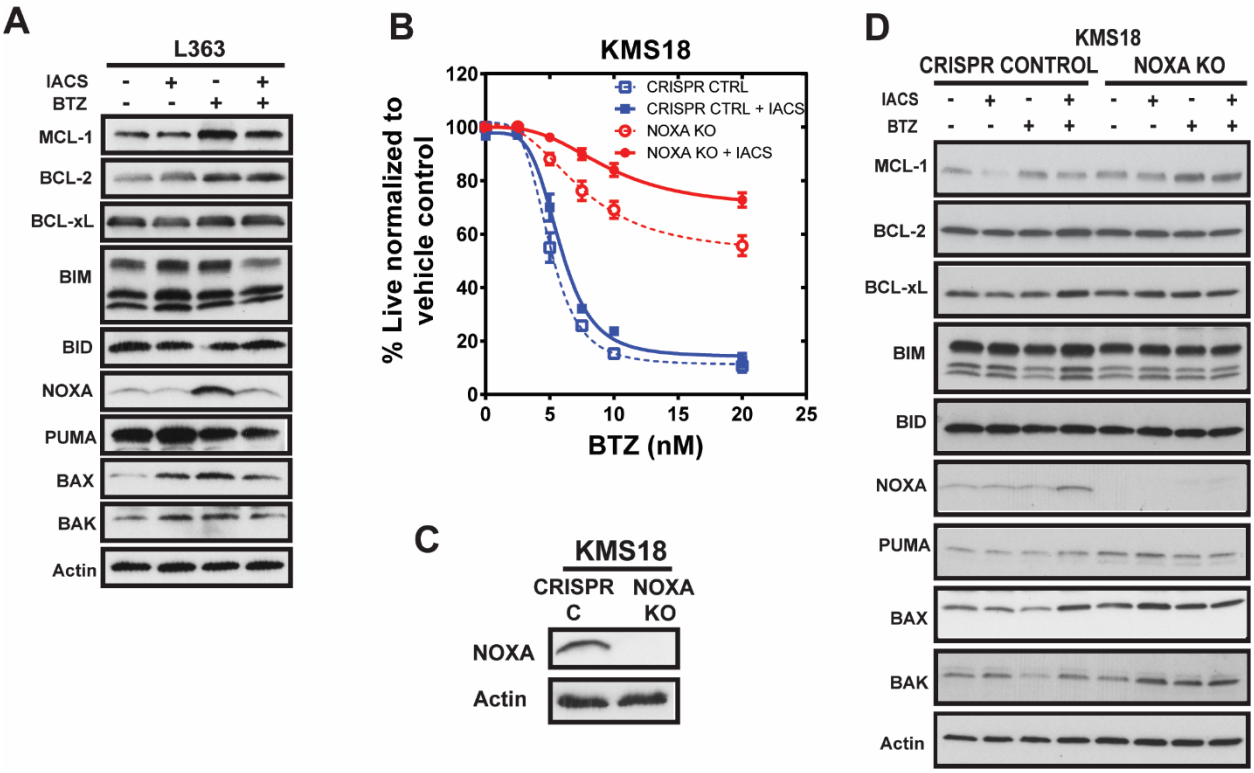

Fig. S7. ETC suppression promotes resistance to BTZ in NOXA KO MM. (A) Expression of BCL-2 family proteins evaluated in L363 cells treated with IACS +/- BTZ for 6 h by immunoblotting using actin as loading control. **(B)** Dose-response curves for co-treatment of KMS18 NOXA KO and CRISPR control cells with 25nM IACS and increasing doses of BTZ for 24 h. Cell viability assessed by AnnexinV/DAPI flow cytometry. Data are represented as mean ± SEM (n = 3). **(C)** Expression of NOXA evaluated in KMS18 NOXA KO and CRISPR control cells by immunoblotting using actin as loading control. **(D)** Expression of BCL-2 family proteins evaluated in KMS18 control and NOXA KO cells treated with IACS +/- BTZ for 6 h by immunoblotting using actin as loading control.

Fig S8

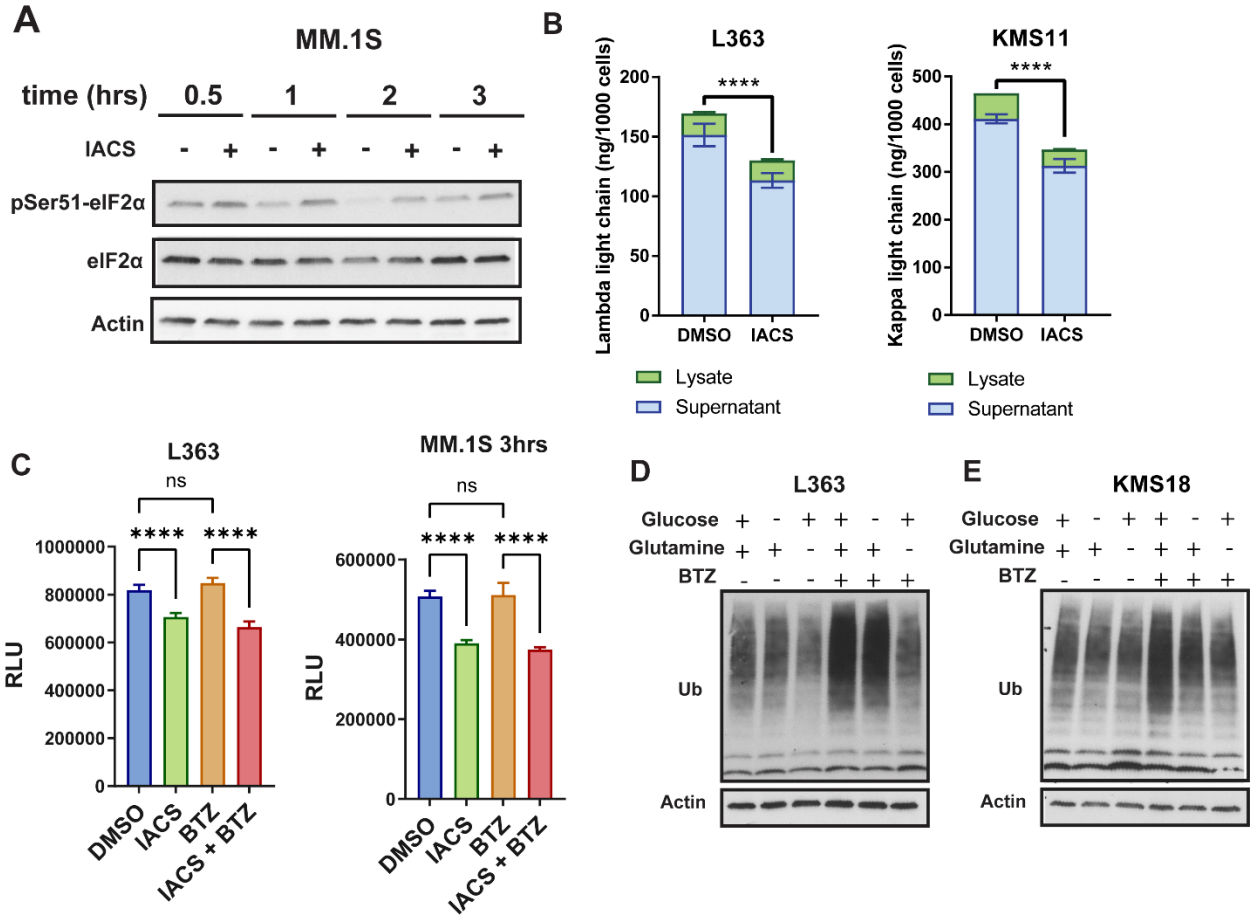

Fig. S8. IACS treatment induces early upregulation of eIF2α phosphorylation in MM.1S cells. (A) Expression of pSer51-eIF2α and total eIF2α evaluated in MM.1S cells treated with IACS by immunoblotting using actin as loading control. **(B)** Intracellular and secreted lambda and kappa light chain antibody levels were measured in L363 and KMS11 cells, respectively, treated with 25nM IACS for 24 h. Data is presented as mean ± SD (n = 6). Adjusted p values are calculated using a two-way ANOVA with post-hoc Sidak's multiple comparisons test. **(C)** ATP levels in L363 and MM.1S upon IACS (25nM) or BTZ (6nM) or the combination treatment using a CellTiter-Glo luminescence assay and presented as relative luminescence units (RLU) compared to the control. Data are represented as mean ± SEM (n = 3). Adjusted p-values are calculated using Tukey's multiple comparisons test. Expression of ubiquitinated proteins in **(D)** L363 and **(E)** KMS18 cells cultured with/without glucose or glutamine +/- BTZ for 6 h evaluated by immunoblotting using actin as loading control.

Fig S9

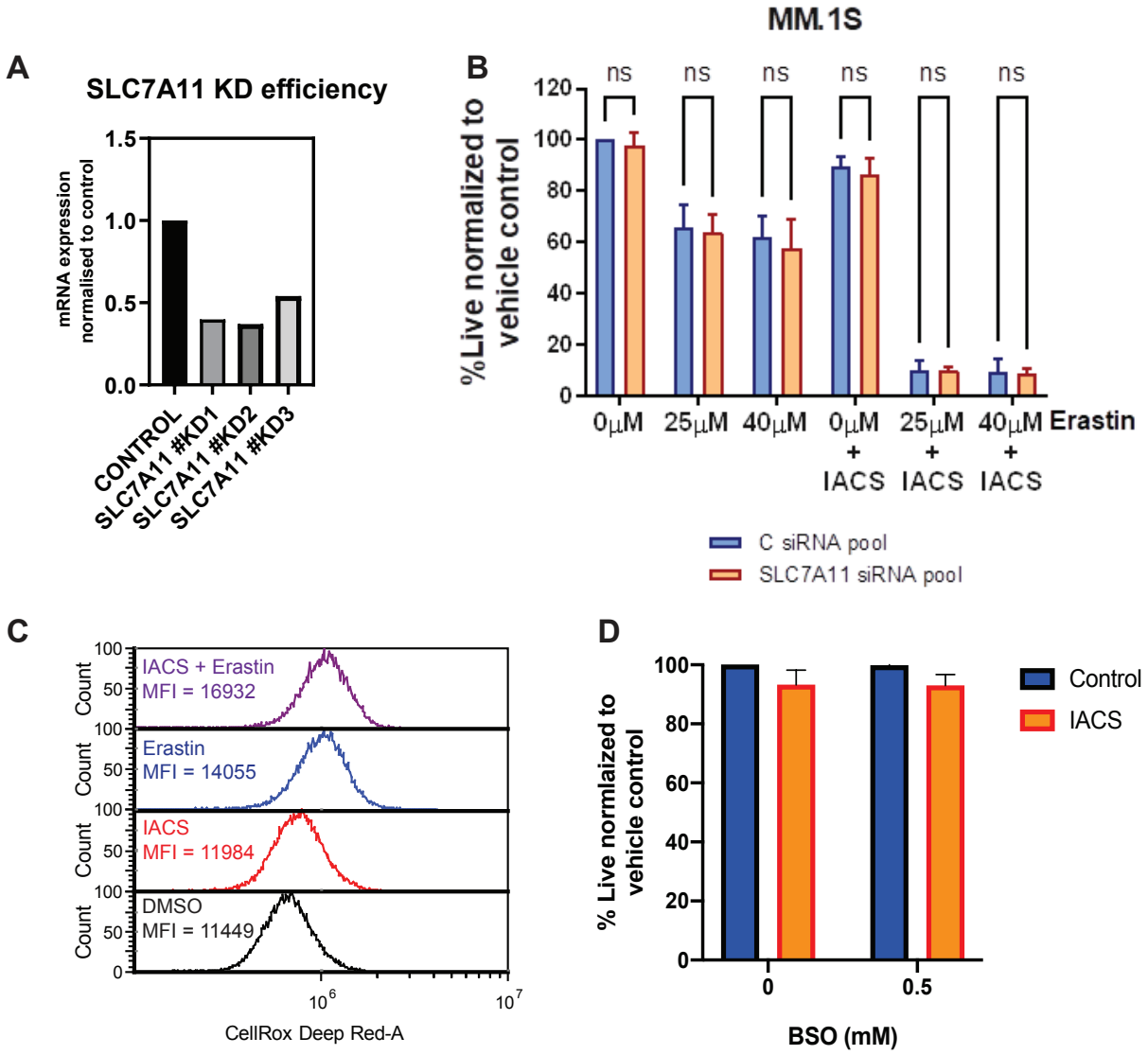

Fig. S9. Erastin increases cellular ROS and decreases MM cell viability in a potentially non-SLC7A11 dependent manner. (A) SLC7A11 RNA expression quantified in 3 KDs in L363 cells by qRT PCR normalized to control. **(B)** Control siRNA or SLC7A11 siRNA transfected MM.1S cells were treated with IACS (25nM), erastin (25μM and 40μM) or the combination for 24 h and cell viability assessed by AnnexinV/DAPI flow cytometric staining. n = 3 independent experiments. Data are presented as mean ± SD. **(C)** Cellular ROS levels in L363 cells treated with 25nM IACS +/- 25μM erastin for 24 h using CellROX Deep Red. One representative experiment is shown (n = 3). **(D)** L363 cells treated with DMSO or 0.5 mM BSO for 24 hrs evaluated for viability by Annexin V/DAPI flow cytometric staining, n=3. Data are presented as mean values ± SD.

Fig S10

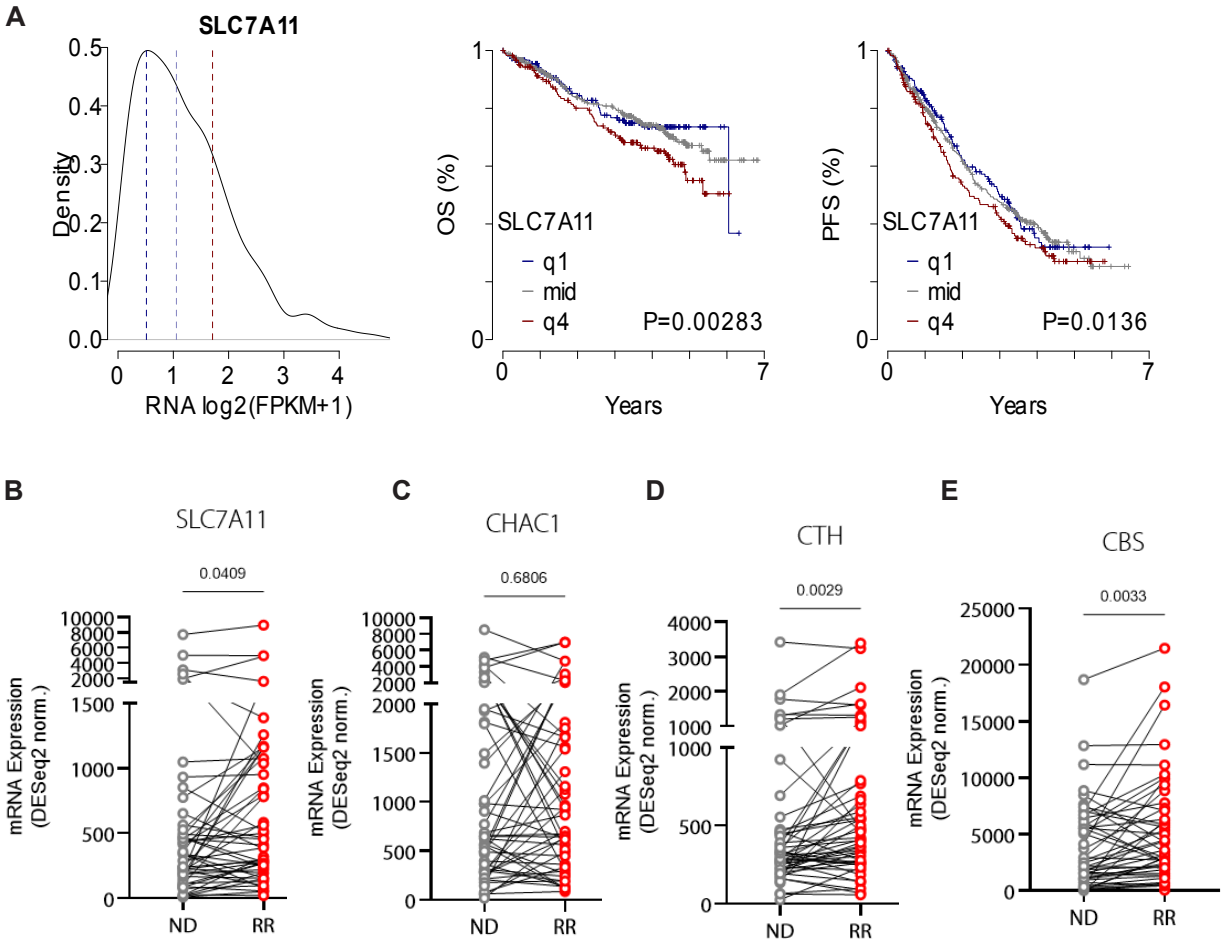

Fig. S10. Association of SLC7A11 with MM PFS and OS and expression of SLC7A11, CHAC1, CTH, and CBS in paired ND and RR MM. (A) (left) Expression of *SLC7A11* in newly diagnosed samples from the CoMMpass study treated with front-line proteasome inhibitors (N=725). First, second, and third quartiles are denoted by blue, gray, and red, dashed vertical lines, respectively. Association of *SLC7A11* expression and OS (middle) and PFS (right) in CoMMpass patients with the patients stratified by *SLC7A11* expression into a low quartile (q1, blue), the two middle quartiles (mid, gray), and high quartile (q4, red) shown. Significance was determined using a Cox proportional hazards model with a Wald's test where gene expression was treated as a quantitative response. **(B)** *SLC7A11*, **(C)** *CHAC1* **(D)** *CTH* and **(E)** *CBS* gene expression in ND vs RR samples. P-value calculated by Wilcoxon matched-pairs signed rank test.

Fig S11

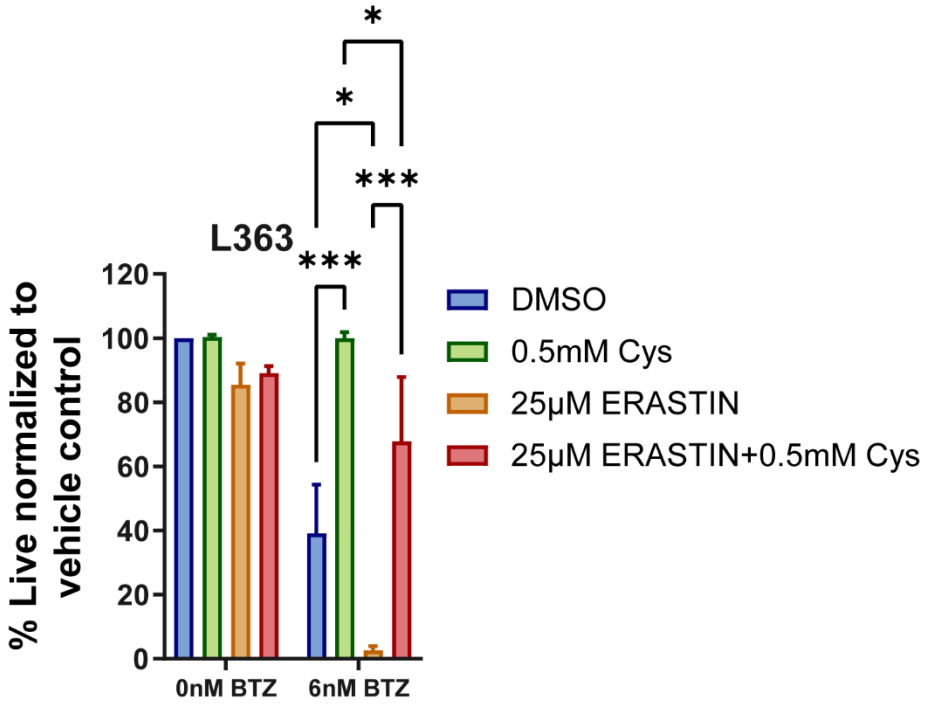

Fig. S11. Erastin increases sensitivity to BTZ that is reversed upon cysteine supplementation. L363 cells treated with 6nM BTZ, 25μM erastin and the combination were supplemented with 0.5mM Cys for 24hrs followed by evaluation of cell viability by Annexin V/DAPI flow cytometric staining. Data are represented as mean ± SEM (n = 2). Adjusted p-values are calculated using a two-way ANOVA with Tukey's multiple comparisons test.

Fig S12

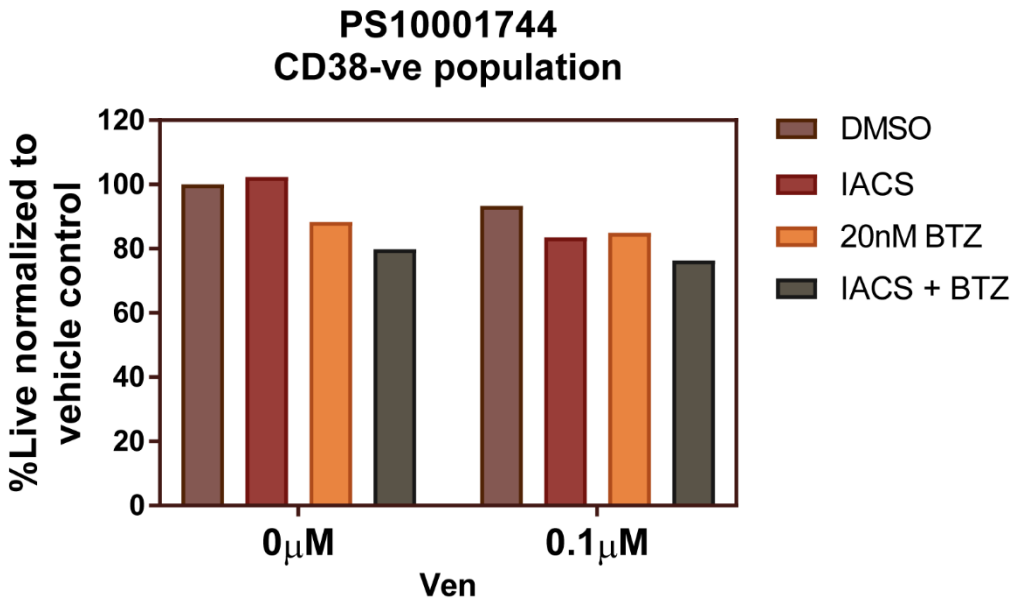

Fig. S12. Venetoclax and BTZ do not impact the viability of non-myeloma normal cellular populations contained in patient bone marrow aspirates Cells gated on CD38 -ve population were analyzed in PS10001744. Aspirates were treated with 25nM IACS, 10nM BTZ or the combination as indicated. Cell viability was assessed by AnnexinV flow cytometric staining.

S. No.	PS ID	IC50 (nM)		FISH
		BTZ	BTZ + IACS	
1	PS10002001	N.D.	N.D.	+1q, +3, +7, +9, +11, -13, +14q, -16q
2	PS10002003	3.076	10.4	+1q, +9, +11, -13
3	PS10002013	6.134	25.86	t(11;14), del(13q)
4	PS10001774	13.74	18.95	t(14;16), +1q, +3, +7, +9, +11, +14q, +17
5	PS10002005	2.305	3.384	+1q, +7, del(13q), +14q
6	PS10002034	3.152	4.442	t(11;14), del(13q)
7	PS10001865	12.64	14.03	+1p, +1q, +3, +7, +9, +11, del(17p), +17
8	PS10001844	251.4	1474	t(11;14), +1q, -13, del(17p)

**N.D. denotes IC50 values were not determined*

Table S1. Characteristics of myeloma patients

Data set title:

Sharma, A et.al ETC suppression antagonizes proteasome inhibitors